How planar optical waves can be made to climb dielectric steps

Manfred Hammer*, Andre Hildebrandt, Jens Förstner

Theoretical Electrical Engineering, University of Paderborn, Germany

We show how to optically connect guiding layers at different elevations in a 3-D integrated photonic circuit. Transfer of optical power carried by planar, semi-guided waves is possible without reflections, without radiation losses, and over large vertical distances. This functionality is realized through simple step-like folds of high-contrast dielectric slab waveguides, in combination with oblique wave incidence, and fulfilling a resonance condition. Radiation losses vanish, and polarization conversion is being suppressed, for TE wave incidence beyond certain critical angles. This can be understood by fundamental arguments resting on a version of Snell's law. The two 90-degree corners of a step act as identical partial reflectors in a Fabry-Perot-like resonator setup. By selecting the step height, i.e. the distance between the reflectors, one realizes resonant states with full transmission. Rigorous quasi-analytical simulations for typical silicon/silica parameters demonstrate the functioning. Combinations of several step junctions can lead to other types of optical on-chip connects, e.g. u-turn- or bridge-like configurations.

The field of silicon photonics [1, 2] holds promise for 3-D integration [3, 4] with compact, high-contrast dielectric optical waveguides at different levels of photonic chips. This might concern small vertical distances, such that evanescent coupling between overlapping components becomes possible, but just as well optically well separated waveguides at larger vertical separations. The latter scenario then raises the question of how to transfer optical power between these distant layers. Conventional evanescent wave coupling [5] either leads to devices measured in centimeters, for vertical distances still below a few hundreds of nanometers [5], or to shorter devices, but then for a separation of not more than a few tens of nanometers [6]. More involved concepts for vertical coupling include waveguides with specifically tapered cores [7, 8], radiative power transfer through grating couplers [9], or even resonant interaction through vertically stacked microrings [10].
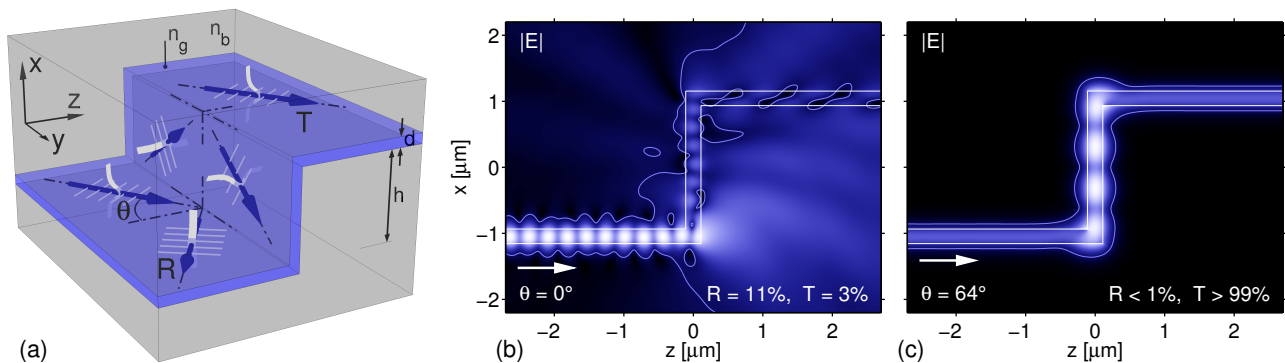

Figure 1: Oblique incidence of semi-guided waves on a step configuration at angle θ: schematic (a), and cross-section views of the optical electric field (absolute value $|\boldsymbol{E}|$, contour at 10% of the maximum field, the colorbar of Figure 2(e) applies), for normal incidence (b), and at angle $\theta = 64°$ (c). Parameters: refractive indices $n_g = 3.45$ (slab cores) : $n_b = 1.45$ (cladding), slab thickness $d = 220\,nm$, vertical slab distance $h = 1.868\,\mu m$, incidence of TE polarized waves at vacuum wavelength $\lambda = 1.55\,\mu m$.

Suppose that, given the task to connect guiding layers at different distant levels in this context of 3-D silicon photonics, and being lured by the strong confinement properties of the high-contrast waveguides, one comes up with the — at a first glance perhaps slightly "naive" — approach of preparing a step-like structure as shown in Figure 1(a), consisting of two sharp 90°-corners with a vertical slab segment in-between. As indicated in the schematic, the structure is assumed to be constant along the y-axis, with half infinite slabs parallel to the y-z plane. If operated in a standard 2-D setting with incidence of vertically (x-) guided, laterally (y-) non-guided plane waves propagating in the positive z-direction normal to the interfaces, this structure clearly fails in view

* University of Paderborn, FG Theoretical Electrical Engineering   *Warburger Str. 100, 33098 Paderborn, Germany*
Phone: ++49(0)5251/60-3560   Fax: ++49(0)5251/60-3524   *E-mail: manfred.hammer@uni-paderborn.de*

of the aforementioned task. Our simulation predicts a transmittance of merely $T = 3\%$ and a reflectance of $R = 11\%$. Most of the power is lost to radiation, and thus must be suspected as a potential source of unwanted crosstalk. Figure 1(b) shows the pronounced radiation losses.

It might thus come as a surprise that the same step structure transfers *all* of the incident optical power to the upper level, if only the in-plane angle of incidence θ is set to $64°$. A respective simulation predicts the profile of Figure 1(c), with all fields nicely confined around the cores, and numerically perfect values of reflectance $R < 1\%$ and transmittance $T > 99\%$. It is the purpose of this letter to highlight this effect, and to provide a basic physical explanation. We refer to a more technical account [11] for details on the theoretical description and related studies. For all simulations in this paper we could rely on a rigorous, semi-analytical solver (vectorial quadridirectional eigenmode propagation, vQUEP) [12, 13, 14] for the vectorial 2-D problems. Figure 1 introduces parameters typical for a silicon photonics platform [15].

For a clarification of the full transmission effect it is instrumental to look at a single corner first, as in Figure 2(a). One notices that the structure is constant along the y-axis. We assume that the slabs are single mode, supporting fundamental guided modes TE_0, TM_0 of both polarizations. For the parameters of Figure 1, these are slab modes with effective mode indices $N_{TE0} = 2.823$, $N_{TM0} = 2.040$.
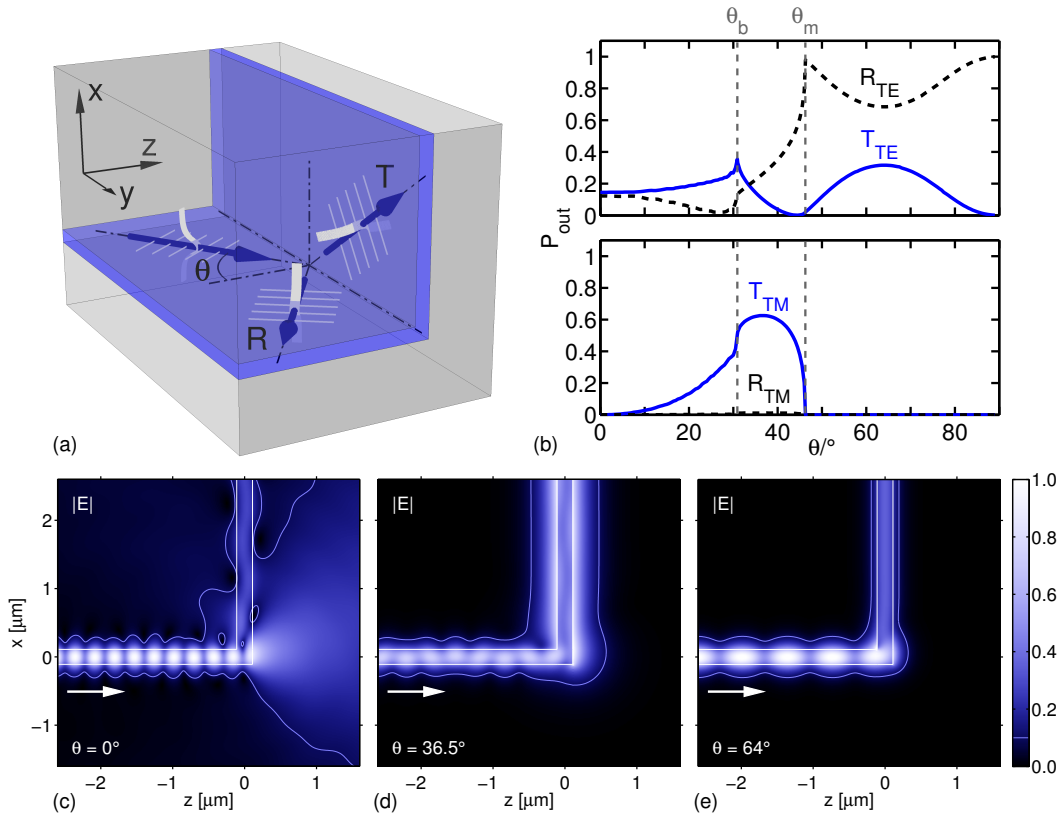

Figure 2: A linear $90°$ waveguide corner at oblique incidence: (a) schematic, (b) modal reflectances R_{TE}, R_{TM} and transmittances T_{TE}, T_{TM} versus the angle of incidence θ (TE_0 and TM_0 modes), and field profiles (absolute value $|\boldsymbol{E}|$ of the electric field, contour at 10% of the field maximum) for angles of incidence $\theta = 0°$ (c), $\theta = 36.5°$ (d), and $\theta = 64°$ (e). See the caption of Figure 1 for parameters.

The TE_0 mode is being sent towards the corner at angle θ. The incoming field thus exhibits an exponential dependence $\sim \exp(-\mathrm{i}k_y y)$ with given wavenumber $k_y = k\, N_{TE0} \sin\theta$ for vacuum wavenumber k. Aiming at a solution of the homogeneous Maxwell equations in the frequency domain, we may restrict the y-dependence of all fields to this single spatial Fourier component. Consequently, any outgoing mode, with effective index N_{out} and travelling at angle θ_{out} versus the x-z-plane, also shares this y-dependence. This can be stated in the form of Snell's law:

$$N_{out} \sin\theta_{out} = N_{TE0} \sin\theta. \tag{1}$$

We look at outgoing TE_0 waves with $N_{out} = N_{TE0}$ first. For the reflected wave Eq. (1) simply gives the law of reflection. The transmitted wave travels upward in the x-y-plane, guided by the vertical slab, at an angle θ. For outgoing TM_0 waves with $N_{out} = N_{TM0} < N_{TE0}$, one needs to distinguish between two cases. Eq. (1) defines

an angle θ_{out} only if $\sin\theta\, N_{\text{TE0}}/N_{\text{TM0}} \leq 1$, i.e. for small angles of incidence $\theta \leq \theta_{\text{m}}$ below a critical angle θ_{m} with $\sin\theta_{\text{m}} = N_{\text{TM0}}/N_{\text{TE0}}$, here $\theta_{\text{m}} = 46.27°$. Reflected and transmitted TM_0 waves then leave the corner region at angles θ_{out} given by Eq. (1).

For excitation at higher angles $\theta > \theta_{\text{m}}$, however, Eq. (1) does not apply. Any TM wave excited in the vicinity of the corner has to satisfy the local wave equation [16] with the externally enforced y-dependence. It does so by compensating the too-large wavenumber k_y by an imaginary wavenumber in the direction of the outward axis ($-z$ for the reflected wave, x for the transmitted wave), i.e. the wave becomes evanescent, what concerns propagation in the x-z-plane. For $\theta > \theta_{\text{m}}$ one observes only outgoing TE waves "far away" from the corner.

Apart from the two guided modes, a continuum of nonguided modes with oscillatory behaviour in the cladding region, and with effective mode indices $N_{\text{out}} \leq n_{\text{b}}$ below the upper limit of the background refractive index n_{b} ("cladding modes"), can be associated with the horizontal and vertical slabs. Applying the former arguments to the modes of this radiation continuum, one finds that all of these modes become x-z-evanescent, if $\sin\theta\, N_{\text{TE0}}/n_{\text{b}} \geq 1$. Consequently, all radiation losses vanish for $\theta > \theta_{\text{b}}$ with $\sin\theta_{\text{b}} = n_{\text{b}}/N_{\text{TE0}}$, here $\theta_{\text{b}} = 30.91°$. Note that the reasoning on the critical angles (cf. Ref. [11] for a more formal and more general account) depends on the properties of the outgoing slab waveguides only, irrespectively of e.g. the corner shape (rounding), or of the corner angle.

Similar arguments apply for plane-wave scattering from cylinders at oblique incidence [17, 18], for slab waveguides with straight discontinuities, typically end facets, with oblique incidence of guided modes, [19, 20, 21, 16], and for slab waveguides with periodic corrugations at oblique incidence [22, 23]. So far, however, we've not encountered this reasoning in case of non-coplanar slabs. When adapted to the present configurations, the frequency-domain Maxwell equations coincide formally with the equations that govern the modes of 3-D channel waveguides, where the present wavenumber k_y takes the role of the propagation constant; the problems differ with respect to boundary conditions [16]. The suppression of radiation losses can then be understood in terms of an angle-dependent, negative effective permittivity [11, 16]. The same effect enables the formation of guided modes in channel waveguides with 2-D confinement.

Figure 2(b) shows the power transmission properties of the corner structure, concerning the fundamental guided modes, as a function of the angle of incidence. The critical angles θ_{b} and θ_{m} are indicated. At normal incidence $\theta = 0$, the otherwise vectorial equations split into the standard scalar 2-D Helmholtz problems for TE and TM waves; there is thus no polarization conversion. The moderate transmittance and reflectance levels of $T_{\text{TE}} = 14\%$, $R_{\text{TE}} = 13\%$, $T_{\text{TM}} = R_{\text{TM}} = 0$ relate to pronounced radiation losses, clearly evident in the field profile in Figure 2(c).

Radiation losses, and thus all fields outside the evanescent tails around the slab cores, vanish for wave incidence at angles beyond θ_{b}. Strong polarization conversion is observed, with an extremal value of TM transmission at $\theta = 36.5°$ with transmittance and reflectance levels of $T_{\text{TE}} = 10\%$, $R_{\text{TE}} = 26\%$, $T_{\text{TM}} = 63\%$, and $R_{\text{TM}} = 1\%$. The reflected guided waves of both polarizations lead to a slightly irregular beating pattern of the partly standing, partly traveling waves in the horizontal slab (cf. Figure 2(d)). In the vertical slab, the strong TM contribution manifests in the large electric fields immediately outside the core (the absolute value $|\boldsymbol{E}|$ of the electric field vector is shown). Upward traveling TE and TM waves, with unequal amplitudes, cause a weak beating pattern, barely visible in the figure.

The polarization conversion is suppressed at even higher angles of incidence for $\theta > \theta_{\text{m}}$. The field profile in panel (e) of Figure 2, for incidence at $\theta = 64°$ with extremal levels $T_{\text{TE}} = 32\%$, $R_{\text{TE}} = 68\%$, $T_{\text{TM}} = R_{\text{TM}} = 0$, shows a tight field confinement around the slab cores. Note that this is still a vectorial problem where TM waves play a role in the solution; their contribution, however, remains restricted to the immediate vicinity of the corner, here at the origin, due to their x-z-evanescent behaviour.

Having thus clarified some properties of the constituting corners, we now resume the discussion of the step structure. With a view to the aim of large power transfer, we select the angle of incidence $\theta = 64°$ that leads to the TE transmission maximum of the separate corners. All former arguments on suppression of radiation losses, and on suppression of polarization conversion, rely on the properties of the outgoing slabs only, without any reference to the particular shape of the structure that connects these outlets. We can thus expect, at this angle of incidence, and for identical slab properties, that neither radiation losses nor conversion to TM occur when the step is being excited by the TE_0 wave.

Further we assume that the intermediate vertical segment is of sufficient height h, such that any x-z-evanescent

fields (of either TE or TM polarization), that are being excited at one of the corner points, are negligible in the region around the respective other corner. Then only the upward and downward travelling TE_0 waves remain that mediate between the corners. These waves and the incoming, reflected, and transmitted TE_0-waves in the horizontal slabs all propagate at the same angle θ with respect to the x-z-plane. They share the uniform harmonic y-dependence, which can then be disregarded for the discussion of the propagation along the slab cores.

Consequently, we may view the step as a system of two identical partial reflectors, the corners, with counter-propagating waves of a single polarization in between, i.e. as a system akin to a Fabry-Perot-interferometer [24]. Here the step height h plays the role of the distance between the two reflectors. Accordingly, the scan over h in Figure 3 reveals a regular series of resonances. One of the extremal states with full transmission has been selected for the example in Figure 1(c).
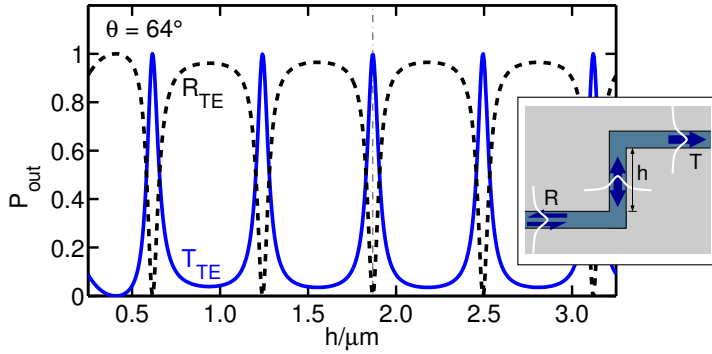

Figure 3: For the step configuration of Figure 1(a): transmittance T_{TE} and reflectance R_{TE} as a function of the step height h. The indicated level $h = 1.868\,\mu m$ relates to Figure 1(b, c).

For sufficiently large h, say for $h > 0.75\,\mu m$, maxima in T_{TE} with unit transmittance appear regularly at distances of $\Delta h = \lambda/(2N_{TE0}\cos\theta) = 626\,nm$. Here $kN_{TE0}\cos\theta$ is the wavenumber component relevant for the propagation in the $\pm x$ direction. Originating from a resonance effect, these states depend more or less critically on all parameters that enter. Concerning the step height h, in Figure 3 one observes levels $T_{TE} > 99\%\,|\,90\%\,|\,75\%\,|\,50\%$ for intervals of full width $\Delta h = 8\,nm\,|\,25\,nm\,|\,44\,nm\,|\,77\,nm$ around the peak centers. Considering the operation wavelength as a further example, respective simulations show transmittance levels $T_{TE} > 99\%\,|\,90\%\,|\,75\%\,|\,50\%$ for spectral intervals of widths $\Delta\lambda = 4\,nm\,|\,13\,nm\,|\,23\,nm\,|\,40\,nm$, centered around the design wavelength $\lambda = 1.55\,\mu m$. The 50%-transmittance window thus covers the entire C-band of infrared optical communications. Note that radiation losses and polarization conversion are fully suppressed within the given intervals; the non-transmitted part of the incident power is reflected as a semi-guided TE_0-wave.

Beyond the selection of a corner configuration with high transmission, and the height scan in Figure 3, no particular optimization has been necessary to identify step configurations with good performance. Within certain limits, this procedure can be reversed into an approach of fixing a step height first, followed by an angular scan. Nevertheless, there is plenty of room left for further optimization, aiming e.g. at lossless corner configurations with higher transmittance. This should lead to steps with less critical resonance conditions, i.e. with improved spectral tolerances, and generally relaxed tolerance requirements. Further studies could also investigate the incidence of TM waves, and thus configurations where both propagating TE and TM waves connect the corners, in detail. While so far these are evidently quasi 3-D concepts at best, the effect can be transferred to "real" 3-D by considering oblique incidence of laterally wide semi-guided beams with narrow angular spectrum [11].

In conclusion, we have shown that semi-guided planar optical waves *can* be made to climb steps, without radiation losses, polarization conversion, or reflections. This is achieved for simple dielectric slabs, with relatively modest means of oblique incidence, combined with a Fabry-Perot-like resonance effect. One might compare with concepts relying on line defects in photonic crystals [25], on various types of (lossy) plasmonic wave confinement [26], or on specific corner geometries [27] in conventional high-contrast dielectric waveguides.

Extension to some other, perhaps even more intriguing examples is obvious. For sufficient step height, one of the corners in a step can be mirrored without affecting the transmission. Steps can be concatenated, with intermediate slab segments of arbitrary length. Our simulations predict modal transmittance values $T_{TE} > 99\%$ for both structures in Figure 4.
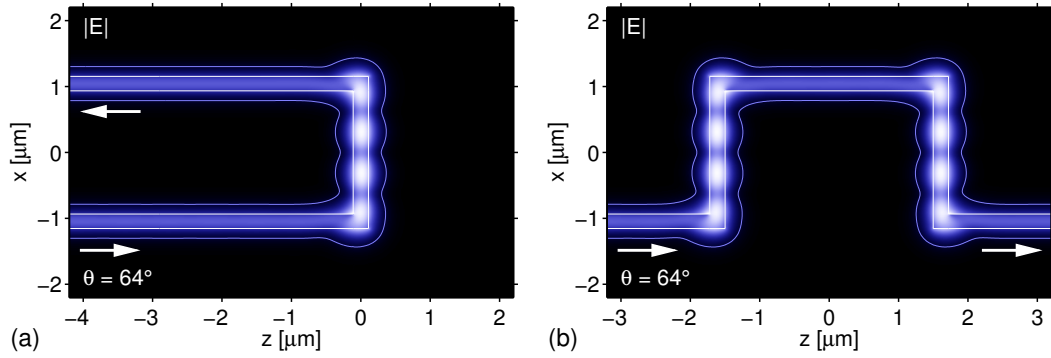
Figure 4: U-turn (a) and bridge configurations (b) with full transmission of semi-guided TE waves at oblique incidence; absolute value $|\mathbf{E}|$ of the optical electric field, contour at 5% of the maximum level, cf. the colorbar of Figure 2(e). Parameters are as in Figure 1(c), with a $3\,\mu m$ slab segment as the upper level of the bridge (b).

Acknowledgments

References

[1] R. Soref. The past, present, and future of silicon photonics. *IEEE Journal of Selected Topics in Quantum Electronics*, 12(6):1678–1687, 2006.

[2] P. Koonath, T. Indukuri, and B. Jalali. Monolithic 3-D silicon photonics. *Journal of Lightwave Technology*, 24(4):1796–1804, 2006.

[3] P. Prakash Koonath and B. Jalali. Multilayer 3-D photonics in silicon. *Optics Express*, 15(20):12686–12691, 2007.

[4] N. Sherwood-Droz and M. Lipson. Scalable 3D dense integration of photonics on bulk silicon. *Optics Express*, 19(18):17758–17765, 2011.

[5] R. A. Soref, E. Cortesi, F. Namavar, and L. Friedman. Vertically integrated silicon-on-insulator waveguides. *IEEE Photonics Technology Letters*, 3(1):22–24, 1991.

[6] J. K. Doylend, A. P. Knights, C. Brooks, and P. E. Jessop. CMOS compatible vertical directional coupler for 3D optical circuits. In *Proceedings of SPIE*, volume 5970, pages 59700G–10, 2005.

[7] R. Sun, M. Beals, A. Pomerene, J. Cheng, C.-Y. Hong, L. Kimerling, and J. Michel. Impedance matching vertical optical waveguide couplers for dense high index contrast circuits. *Optics Express*, 16(16):11682–11690, 2008.

[8] J. F. Bauters, M. L. Davenport, M. J. R. Heck, J. K. Doylend, A. Chen, A. W. Fang, and J. E. Bowers. Silicon on ultra-low-loss waveguide photonic integration platform. *Optics Express*, 21(1):544–555, 2013.

[9] P. Dong and A. G. Kirk. Compact grating coupler between vertically stacked silicon-on-insulator waveguides. In *Proceedings of SPIE*, volume 5357, pages 135–142, 2004.

[10] J. T. Bessette and D. Ahn. Vertically stacked microring waveguides for coupling between multiple photonic planes. *Optics Express*, 21(11):13580–13591, 2013.

[11] M. Hammer, A. Hildebrandt, and J. Förstner. Full resonant transmission of semi-guided planar waves through slab waveguide steps at oblique incidence, 2015. arXiv:1502.07619 [physics.optics].

[12] M. Hammer. Oblique incidence of semi-guided waves on rectangular slab waveguide discontinuities: A vectorial QUEP solver. *Optics Communications*, 338:447–456, 2015.

[13] M. Hammer. Quadridirectional eigenmode expansion scheme for 2-D modeling of wave propagation in integrated optics. *Optics Communications*, 235(4–6):285–303, 2004.

[14] M. Hammer. METRIC — Mode expansion tools for 2D rectangular integrated optical circuits. http://metric.computational-photonics.eu/.

[15] W. Bogaerts, R. Baets, P. Dumon, V. Wiaux, S. Beckx, D. Taillaert, B. Luyssaert, J. Van Campenhout, P. Bienstman, and D. Van Thourhout. Nanophotonic waveguides in silicon-on-insulator fabricated with CMOS technology. *Journal of Lightwave Technology*, 23(1):401–412, 2005.

[16] F. Çivitci, M. Hammer, and H. J. W. M. Hoekstra. Semi-guided plane wave reflection by thin-film transitions for angled incidence. *Optical and Quantum Electronics*, 46(3):477–490, 2014.

[17] J. R. Wait. Scattering of a plane wave from a circular dielectric cylinder at oblique incidence. *Canadian Journal of Physics*, 33(5):189–195, 1955.

[18] H. Wang and G. Nakamura. The integral equation method for electromagnetic scattering problem at oblique incidence. *Applied Numerical Mathematics*, 62(7):860–873, 2012.

[19] S.-T. Peng and A. Oliner. Guidance and leakage properties of a class of open dielectric waveguides: Part I — mathematical formulations. *IEEE Transactions on Microwave Theory and Techniques*, MTT-29(9):843–854, 1981.

[20] T. P. Shen, R. F. Wallis, A. A. Maradudin, and G. I. Stegeman. Fresnel-like behavior of guided waves. *Journal of the Optical Society of America A*, 4(11):2120–2132, 1987.

[21] W. Biehlig and U. Langbein. Three-dimensional step discontinuities in planar waveguides: Angular-spectrum representation of guided wavefields and generalized matrix-operator formalism. *Optical and Quantum Electronics*, 22(4):319–333, 1990.

[22] K. Wagatsuma, H. Sakaki, and S. Saito. Mode conversion and optical filtering of obliquely incident waves in corrugated waveguide filters. *IEEE Journal of Quantum Electronics*, 15(7):632–637, 1979.

[23] J. Van Roey and P. E. Lagasse. Coupled wave analysis of obliquely incident waves in thin film gratings. *Applied Optics*, 20(3):423–429, 1981.

[24] M. Born and E. Wolf. *Principles of Optics, 7th. ed.* Cambridge University Press, Cambridge, UK, 1999.

[25] J. D. Joannopoulos, S. G. Johnson, J. N. Winn, and R. D. Meade. *Photonic Crystals: Molding the Flow of Light, 2nd edition*. Princeton, 2008.

[26] D. K. Gramotnev and S. I. Bozhevolnyi. Plasmonics beyond the diffraction limit. *Nature Photonics*, 4:83–91, 2010.

[27] R. U. Ahmad, F. Pizzuto, G. S. Camarda, R. L. Espinola, H. Rao, and R. M. Osgood. Ultracompact corner-mirrors and T-branches in silicon-on-insulator. *IEEE Photonics Technology Letters*, 14(1):65–67, 2002.